Mean first-passage time to a small absorbing target in three-dimensional elongated domains

Denis S. Grebenkov[1,*] and Alexei T. Skvortsov[2,†]

[1]*Laboratoire de Physique de la Matière Condensée, UMR No. 7643, CNRS, Ecole Polytechnique, IP Paris, 91120 Palaiseau, France*

[2]*Maritime Division, Defence Science and Technology Group, 506 Lorimer Street, Fishermans Bend, Victoria 3207, Australia*

(Received 15 February 2022; accepted 15 April 2022; published 4 May 2022)

We derive an approximate formula for the mean first-passage time (MFPT) to a small absorbing target of arbitrary shape inside an elongated domain of a slowly varying axisymmetric profile. For this purpose, the original Poisson equation in three dimensions is reduced to an effective one-dimensional problem on an interval with a semipermeable semiabsorbing membrane. The approximate formula captures correctly the dependence of the MFPT on the distance to the target, the radial profile of the domain, and the size and the shape of the target. This approximation is validated by Monte Carlo simulations.

DOI: 10.1103/PhysRevE.105.054107

I. INTRODUCTION

The concept of first-passage time, i.e., the time taken for a diffusing particle to arrive at a given location, is very common in describing many natural phenomena. Nowadays, it is widely used in chemistry (geometry-controlled kinetics), biology (gene transcription and foraging behavior of animals), and many applications (financial modeling, forecasting of extreme events in the environment, time to failure of complex devices and machinery, and military operations), see [1–20] and references therein.

Most former works were dedicated to the *mean* first-passage time (MFPT), which is also related the overall reaction rate onto the target region. Since exact formulas for the MFPT are only available for a few special cases of highly symmetric domains (such as a sphere or disk), a variety of powerful methods have been developed. In particular, many approximate solutions were derived in the so-called narrow escape limit when the target size goes to 0 [21–35]. While these asymptotic results are valid for generic domains, their accuracy can be considerably reduced when the confining domain is elongated (e.g., a long truncated cylinder or a prolate spheroid). In this case, the target region can still be very small compared to the diameter of the confining domain (i.e., the size of the domain in the longitudinal direction), but comparable to the size of the domain in the transverse directions. The effect of the confinement anisotropy on the MPFT was studied in [36]. Recently, we proposed a simple yet efficient method for deriving approximate solutions of the MPFT in elongated domains on the plane [37]. The aim of this paper is to extend this method to three dimensions and to derive a general approximate formula for the MFPT in an elongated three-dimensional domain with reflecting boundaries. The shape of the domain is assumed to be axisymmetric, smooth, and slowly varying in the longitudinal direction (without deep pockets and enclaves), but otherwise general. The target is assumed to be small, but also of arbitrary shape. We validate our findings by Monte Carlo simulations.

II. APPROXIMATE SOLUTION

We consider an elongated axisymmetric domain of length ℓ, which is determined by a smooth profile $r(z)$:

$$\Omega = \{(x, y, z) \in \mathbb{R}^3 : x^2 + y^2 < r^2(z), 0 < z < \ell\}. \quad (1)$$

Throughout the paper, we assume that the aspect ratio r_0/ℓ of the domain [with $r_0 = \max\{r(z)\}$] is small and its boundary profile is smooth, $dr(z)/dz \ll 1$. A small absorbing target Γ is located inside the domain at (x_T, y_T, z_T) (see Fig. 1). We assume that the target diameter is much smaller than the width of the cross section at which the target is located: $\mathrm{diam}\{\Gamma\} \ll r(z_T)$.

Similar to planar domains [37], the main analytical formula will be derived by employing a three-step approximation. First, the absorbing target is replaced by an absorbing disk of the same trapping coefficient K; the disk is oriented perpendicular to the symmetry axis of the domain. Far away from the target such a replacement is justifiable because at a distance greater than the size of the target [but still much smaller than $r(z_T)$ and ℓ] the absorption flux can be characterized by the first (monopole) moment of the shape of the target, and this equivalence simply preserves it. The trapping coefficient is proportional to the electrostatic capacitance C of the target, $K = 4\pi DC$, where D is the diffusion coefficient [38,39]. For a variety of shapes (e.g., sphere, ellipsoid, cube, prism, perturbed axisymmetric shapes, or even some fractals objects), capacitance is well known or can be accurately estimated from various approximations, see [39–46] and references therein. For a disk of radius a, the capacitance is $(2/\pi)a$ [43]. Knowing the capacitance C of a given target shape, one can thus easily deduce the radius $a = (\pi/2)C$ of the equivalent absorbing disk.

Second, we introduce the semipermeable semiabsorbing boundary (membrane) across the domain that passes through

*denis.grebenkov@polytechnique.edu

†alex.skvortsov@dst.defence.gov.au

the equivalent absorbing disk, i.e., at $z = z_T$, where z_T is the longitudinal target location. In line with the conventional arguments of effective medium theory, the trapping of the target can approximately be captured by means of this boundary with some effective reactivity κ. A similar approach, often referred to as the lump parameter approximation, has been applied in many areas of physics and engineering (effective acoustic impedance of perforated screens [47], effective electric conductance of lattices and grids [48], and effective boundary condition for porous materials [49–51]). To relate the effective trapping rate of the membrane with the geometrical setting, we assume that the effective trapping rate of the membrane is equal to the trapping flux of the particles induced by the presence of the target,

$$\kappa = \frac{K(r_T)}{S(z_T)}, \tag{2}$$

where $S(z) = \pi r^2(z)$ is the cross-sectional area at height z. We stress that K and thus κ depend on the radial position $r_T = \sqrt{x_T^2 + y_T^2}$ of the target (an equivalent disk) in the cross section of the domain. In other words, the trapping coefficient $K(r_T)$ of the target inside the confining domain is different from its value K_0 in the open space (when $\Omega = \mathbb{R}^3$). Moreover, it is the latter dependence that determines the MFPT properties. Calculation of the position-dependent trapping coefficient K is one of the main ingredients of the proposed method. In the Appendix we proposed the approximation

$$K = K_0 \Psi(a/r(z_T), r_T/r(z_T)), \tag{3}$$

where the function $\Psi(\nu, \eta)$, defined by Eq. (A1), is deduced by interpolating two analytical results for $r_T = 0$ (at the symmetry axis of the domain) and $r_T = R - a$ (near the domain wall). This function accounts for the relative target size $\nu = a/r(z_T)$ and the relative traversal deviation $\eta = r_T/r(z_T)$ of the target from the center of the domain cross section.

Third, after its release at some point in the elongated domain, a Brownian particle frequently bounces from the reflecting walls while gradually diffusing along the domain towards the target. The shape of the walls [defined by $r(z)$] can additionally create the so-called entropic drift, which can either speed up or slow down the arrival at the target [4,11,12]. In any case, the information about the particle's initial lateral location (e.g., across the domain) becomes rapidly irrelevant and the original MFPT problem, governed by the Poisson equation, is essentially reduced to the one-dimensional problem. While the classical Fick-Jacobs equation determines the concentration of particles averaged over the cross section of the tube (see [4,11,12] and references therein), the survival probability is determined by the backward diffusion equation with the adjoint diffusion operator [52]. In particular, the MFPT $T(z)$ in an elongated domain satisfies [4,11–13]

$$\frac{d}{dz}\left[S(z)\frac{dT}{dz}\right] = -\frac{S(z)}{D}. \tag{4}$$

As the results of these approximations, the original problem of finding the MFPT to a small target of arbitrary shape in a general elongated domain is reduced to the one-dimensional problem, which can be solved analytically.

We sketch only the main steps of the solution, while the details in a similar case of planar domains can be found in [37]. We search for the solution of Eq. (4) in the intervals $(0, z_T)$ and (z_T, ℓ). Integrating this equation over z and imposing Neumann (reflecting) boundary conditions at $z = 0$ and $z = l$, we get

$$T(z) = \begin{cases} C_- - \int_0^z dz' \frac{V(z')}{DS(z')}, & 0 < z < z_T \\ C_+ - \int_z^\ell dz' \frac{V(l) - V(z')}{DS(z')}, & z_T < z < \ell, \end{cases} \tag{5}$$

where $V(z) = \int_0^z dz' S(z')$ is the volume of the (sub)domain restricted between 0 and z. The integration constants $C_\pm$ are determined by imposing the effective semipermeable semiabsorbing boundary condition at the target location $z = z_T$,

$$T(z_T - 0) = T(z_T + 0), \tag{6}$$

$$D\left[\frac{dT}{dz}(z_T + 0) - \frac{dT}{dz}(z_T - 0)\right] = \kappa\, T(z_T), \tag{7}$$

where κ is given by Eq. (2). The first relation ensures the continuity of the MFPT, whereas the second condition states that the difference between the diffusion fluxes at two sides of the semipermeable boundary at z_T is equal to the reaction flux on the target (an equivalent disk). The latter flux is proportional to T, with an effective reactivity κ equal to the effective trapping rate of the target [Eq. (2)]. Finally, substituting Eq. (5) into Eqs. (6) and (7), we get the solution of the problem

$$T(z) = \frac{l^2}{D}[U_\sigma(z_T/\ell) - U_\sigma(z/\ell)] + \frac{l}{\kappa}\frac{v(1)}{s(z_T/\ell)}, \tag{8}$$

where we introduced the dimensionless quantities

$$U_-(\zeta) = \int_0^\zeta d\zeta' \frac{v(\zeta')}{s(\zeta')}, \quad U_+(\zeta) = \int_\zeta^1 d\zeta' \frac{v(1) - v(\zeta')}{s(\zeta')}, \tag{9}$$

with

$$\zeta = z/\ell, \quad S(z) = \pi r_0^2 s(z/\ell), \tag{10}$$

$$V(z) = \pi r_0^2 \ell v(z/\ell), \quad v(\zeta) = \int_0^\zeta d\zeta' s(\zeta'). \tag{11}$$

The index σ in Eq. (8) is the sign of $z - z_T$, i.e., $\sigma = +$ for $z > z_T$ and $\sigma = -$ for $z < z_T$. For a given profile $r(z)$, all these functions can be easily computed either analytically (see examples in Table I) or numerically. In the simplest case of the cylindrical domain, $r(z) = r_0$, we simply get

$$T(z) = \begin{cases} \frac{z_T^2 - z^2}{2D} + \frac{\ell}{\kappa}, & 0 \leqslant z \leqslant z_T \\ \frac{(z - z_T)(2\ell - z_T - z)}{2D} + \frac{\ell}{\kappa}, & z_T \leqslant z \leqslant \ell. \end{cases} \tag{12}$$

Equation (8) is the main result of the paper. As for the case of planar domains [37], this equation consists of two terms. The first (diffusion) term is independent of the size of the target and is related to the time required for a Brownian particle to arrive at the proximity of the target from its initial position. For this reason, the contribution of this term is small when $z \approx z_T$, i.e., when the particle's initial position is near the target. The second (reaction) term in Eq. (8) describes the particle absorption by the target when the particle starts in its vicinity. As it is inversely proportional to the target size, this

TABLE I. Three examples of symmetric elongated domains defined by setting $r(z) = r_0\rho(z/\ell)$, where $\rho(\zeta)$ is the rescaled radial profile ($\zeta = z/\ell$), ℓ is the length of the domain, and $r_0 = \max\{r(z)\}$; $v(\zeta)$ is the rescaled volume in Eq. (11); the functions $U_\pm(\zeta)$ are given in Eq. (9); and the constant c_0 and function $c(\zeta)$ are given by Eq. (15). Other examples can be deduced from similar expressions for the planar case [37] due to the identity $\rho^2(\zeta) = h(\zeta)$ between the rescaled profile $\rho(\zeta)$ of a three-dimensional domain and the rescaled profile $h(\zeta)$ of the analogous two-dimensional domain.

Domain	$\rho(\zeta)$	$v(\zeta)$	$U_-(\zeta)$	$U_+(\zeta)$	c_0	$c(\zeta)$
cylinder	1	ζ	$\frac{1}{2}\zeta^2$	$\frac{1}{2}(1-\zeta)^2$	$\frac{1}{3}$	$1-\zeta$
cone	ζ	$\frac{1}{3}\zeta^3$	$\frac{1}{6}\zeta^2$	$\frac{2-3\zeta+\zeta^3}{6\zeta}$	$\frac{1}{15}$	$\frac{1-\zeta}{3\zeta}$
paraboloid	ζ^2	$\frac{1}{5}\zeta^5$	$\frac{1}{10}\zeta^2$	$\frac{3\zeta^5-5\zeta^3+2}{30\zeta^3}$	$\frac{1}{35}$	$\frac{1-\zeta^3}{15\zeta^3}$

term dominates in the limit of very small targets. We note that the dependence on the lateral width of the domain comes only through the parameter κ.

In many applications, the starting point is not fixed but uniformly distributed inside the domain. In this case, one often uses to the volume-averaged MFPT

$$\overline{T} = \frac{1}{V(l)}\int_0^\ell \pi r^2(z)T(z)dz. \tag{13}$$

By substituting Eq. (8) into this expression we arrive at

$$\overline{T} = \frac{\ell^2}{D}[c_0 + c(z_T/\ell)] + \frac{\ell}{\kappa}\frac{v(1)}{s(z_T/\ell)}, \tag{14}$$

with

$$c_0 = \int_0^1 d\zeta\,\frac{v^2(\zeta)}{v(1)s(\zeta)}, \quad c(\zeta) = \int_\zeta^1 d\zeta'\,\frac{v(1)}{s(\zeta')}. \tag{15}$$

Note also that

$$U_+(\zeta) = c(\zeta) - [U_-(1) - U_-(\zeta)]. \tag{16}$$

III. DISCUSSION

We use Monte Carlo simulations to check the accuracy of the analytical predictions given by Eq. (8) in three geometrical settings illustrated in Fig. 1: (i) a disk of radius ρ in a truncated cylinder, (ii) a cube of edge 2ρ in a truncated cone, and (iii) a sphere of radius ρ in an oscillating profile. The capacitances of these targets are $(2/\pi)\rho$, $(4/3)\rho$ [39,45], and ρ, respectively, from which the radius a of an effective disk takes the values ρ, $(2\pi/3)\rho$, and $(\pi/2)\rho$, respectively. The target is located at $(r_T, 0, \ell/2)$, where $\ell = 5$ is the length of the confining domains. In each simulation run, a particle is released from a random point uniformly distributed in the cross section at $z_0 = 2$. It undertakes independent Gaussian jumps with the standard deviation $\sigma = \sqrt{2D\delta}$ along each coordinate, where $D = 1$ and $\delta = 10^{-6}$ is the time step. The particle is reflected normally on the boundary of the confining domain. The simulation run is stopped when the particle crosses the target. The first-passage time is estimated as $n\delta$, where n is the number of steps until stopping. The MFPT is obtained by averaging over 1000 runs.

The approximate solution for a truncated cylinder is given in Eq. (12), while the general expression (8) is used for two other domains. In the case of a truncated cone $r(z) = a + bz$, the functions $U_\pm(\zeta)$ can also be found explicitly,

$$U_-(\zeta) = \frac{\zeta^2(3+\alpha\zeta)}{6(1+\alpha\zeta)}, \quad U_+(\zeta) = \frac{(1-\zeta)^2(3+2\alpha-\alpha\zeta)}{6(1+\alpha\zeta)},$$

with $\alpha = b\ell/a$. In turn, for an oscillating profile, it is easier to calculate $U_\pm(\zeta)$ directly from their definition (9) via numerical integration.

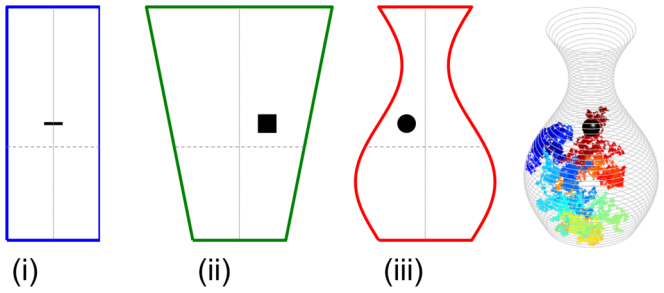

FIG. 1. Projection onto the xz plane of three domains used for Monte Carlo simulations: truncated cylinder, with $r(z) = 1$ (i); truncated cone, with $r(z) = 1 + z/\ell$ (ii); and a domain with an oscillating profile $r(z) = 1 + \frac{1}{2}\sin(2\pi z/\ell)$ (iii), with $\ell = 5$. The vertical dotted line shows the symmetry axis in the z direction ($r = 0$); the horizontal dashed line indicates the location of uniformly distributed starting points (at $z = 2$). A target (in black) is located at $(x_T, 0, \ell/2)$: a disk of radius $\rho = 0.2$ with $x_T = 0$ (i), a cube of edge $2\rho = 0.4$ with $x_T = 0.6$ (ii), and a sphere of radius $\rho = 0.2$ with $x_T = -0.4$ (iii). On the right is an example of a simulated trajectory inside the domain with an oscillating profile, colored from dark blue to dark red according to elapsed time until the first passage to the target (black sphere) at the center.

Figure 2 presents the MFPT as a function of the radial position r_T of the target in the domain. First of all, one can note the overall agreement between our theoretical predictions and Monte Carlo simulations. Both theory and simulations indicate that the MFPT increases when the target is shifted from the center ($r_T = 0$) towards the boundary of the confining domain ($r_T = 0.8$), even though this effect is weak. For a larger spherical target [$\rho = 0.2$, Fig. 2(a)], our approximation slightly underestimates the MFPT in the case (iii) of an oscillating domain; the agreement is better for a smaller target [$\rho = 0.1$, Fig. 2(b)]. The oscillating profile leads to stronger deviations because lateral variations of diffusivity were disregarded [see Eq. (17) below]. The accuracy of this approximation is determined by the average squared amplitude variations of the domain profile, $\frac{1}{\ell}\int_0^\ell dz(dr/dz)^2$. For the three profiles considered (see the caption of Fig. 2), this average takes the following values: 0 for a straight cylinder, $1/\ell^2$ for a truncated cone, and $\pi^2/(2\ell^2)$ for the oscillating profile. The last value is five times higher than that for the truncated cone that explains more noticeable deviations from the theoretical prediction. There are also minor deviations for the case (i) when the disk is close to the boundary. Despite these deviations, we conclude that our three-step approximation accurately captures the properties of the MFPT in elongated domains. Given the simplistic character of this approximation, its accuracy is striking. It is worth stressing that the targets are not too small [e.g., $\rho = 0.2$ is comparable

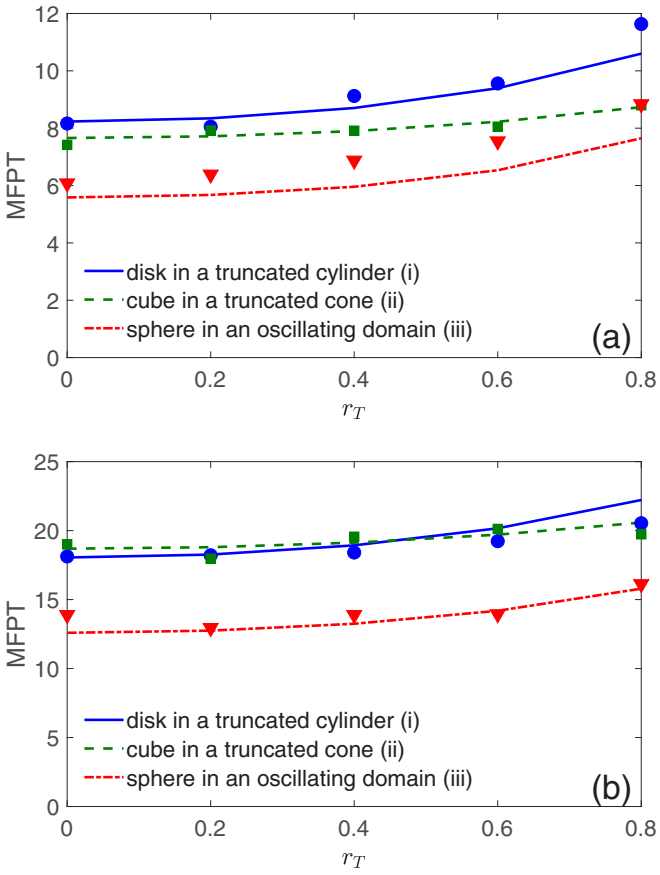

FIG. 2. Mean first-passage time as a function of r_T for diffusion towards a target centered at $\boldsymbol{x}_T = (r_T, 0, \ell/2)$ with (a) $\rho = 0.2$ or (b) $\rho = 0.1$, $D = 1$, $\ell = 5$, the starting point $\boldsymbol{x}_0$ uniform at the cross section at $z_0 = 2$, in three settings shown in Fig. 1: (i) a disk of radius ρ inside a truncated cylinder of radius 1, (ii) a cube of edge 2ρ inside a truncated cone $r(z) = 1 + z/\ell$, and (iii) a sphere of radius ρ inside an oscillating domain $r(z) = 1 + \frac{1}{2}\sin(2\pi z/\ell)$. Lines show theoretical predictions (8); symbols present the mean values from 1000 realizations obtained via Monte Carlo simulations with the time step $\delta = 10^{-6}$.

to the minimal radius of $r(0.75\ell) = 0.5$ of the oscillating domain], the domains are not too elongated (e.g., $r_0/\ell = 0.4$ for the truncated cone), and the particles are released not too far from the target (here $z_T - z_0 = 0.5$ is comparable to the target diameter $2\rho = 0.4$). In other words, even though the assumptions of our approximation are not fully satisfied, its predictions remain in quantitative agreement with Monte Carlo simulations.

IV. CONCLUSION AND PERSPECTIVES

In this paper we obtained a simple formula (8) for the MFPT to a small absorbing target of arbitrary shape in an elongated axisymmetric domain with a slowly changing boundary profile. This formula expresses the MFPT in terms of the dimensions of the domain, the form and the size of the absorbing target, and the target's relative position inside the domain. We validated our analytical predictions by numerical simulations and found excellent agreement. Similar to the planar domains [37], the validity of the proposed framework is grounded in the condition of a slowly changing profile $dr(z)/dz \ll 1$. While the final formula (8) and the main steps of the approximation are very similar to our former results for the planar domain [37], the additional elements developed here are crucial for getting a simple yet accurate formula in three dimensions. The difference between two- and three-dimensional cases becomes apparent from the fact that the analytical framework developed for the planar domain [37] heavily relied on the method of conformal transformations, which is inapplicable in three dimensions. In fact, at each of three approximation steps discussed in Sec. II, the original parameters had to be related to the effective ones; for instance, we needed to determine the radius of an effective disk and to obtain an effective reactivity of the cross section. These relations are not universal and are actually dimension dependent. In particular, the trapping coefficient K, which was known for a target in the plane, had to be obtained in three dimensions (see the Appendix). Its dependence on the target position and relative size is nontrivial and significant (see Fig. 2).

The replacement of an arbitrary three-dimensional target by an absorbing disk was one of the key approximations. There are several ways to rationalize this replacement. (i) From the probabilistic point of view, when the target is small compared to the cross-sectional width of the domain, Brownian motion started sufficiently away from the target has enough time to explore the space around the target in order to "average out" its geometric details. In other words, small targets of different shapes "look" similar to Brownian particles traveling from far away. (ii) In physical terms, the diffusive flux onto a small target can in general be represented via multipole expansions; when the starting point is far away from the target, the lowest-order term is dominant. This so-called monopole approximation has been used in many applications. (iii) Mathematically, the principal eigenvalue of the Laplace operator in a confining domain with a reflecting outer boundary and a small absorbing target is proportional to the capacity of that target, regardless of its shape [53,54]. In summary, when the target is small, its shape does not matter and the disk was chosen as the most convenient shape that allowed us to complete the analysis.

A conventional way of improving the proposed approximation is to account for the next order in the perturbation expansion, which entails introduction of the position-dependent diffusion coefficient [4]

$$D \to \frac{D}{\sqrt{1 + [dr(z)/dz]^2}}. \tag{17}$$

We note that under this approximation the results for the cylindrical domain remain uncharged, while an extension of the main formula (8) is getting more challenging.

Future work may involve an extension of the proposed framework to more complex geometries (an elongated domain with a compound piecewise profile) or an extension to the slightly bent domain (but still with a circular cross section). These extensions are straightforward; the latter case reduces to a simple change of the coordinate z in the main equation (8) to the longitudinal curvilinear coordinate along the bent domain. The generalization of Eq. (8) to domains with a noncircular

cross section is also possible, but is more involved and would require a substantial refinement of the relation (3), while the main equation (8) remains valid.

We believe that the proposed expression for the MFPT is a useful tool for some rapid practical estimations as well as for validation of complex numerical models of particle diffusion in geometrically constrained settings.

ACKNOWLEDGMENTS

D.S.G. acknowledges partial financial support from the Alexander von Humboldt Foundation through a Bessel Research Award. A.T.S. thanks Paul A. Martin for many helpful discussions.

APPENDIX: EFFECTIVE TRAPPING COEFFICIENT FOR AN ABSORBING DISK INSIDE A TUBE

In this Appendix we derive an approximate expression for the trapping coefficient K of a small disk of radius a in a reflecting tube with the cross-sectional area $S(z) = \pi r^2(z)$. For planar domains, the expression for K can be deduced analytically [37]. Unfortunately, there is no closed-form analytical solution for K in the case of a general position of the absorbing disk in a three-dimensional tube with reflecting walls (we note that the classical results for the capacitance of a small conductor in a tube [55–57] correspond to the Dirichlet boundary condition on the tube wall). Nevertheless, there are some analytical results that can be used to conjecture an accurate interpolating solution.

The trapping coefficient K_0 of a target in the whole space $\mathbb{R}^3$ is determined by its capacitance C_0, which depends exclusively on the target shape and thus represents its intrinsic geometric property. However, the presence of the reflecting boundary of a confining domain changes the Brownian dynamics and thus modifies the trapping coefficient. This modification is similar to a change of the capacitance of a small conductor due to the presence of the reflecting boundary. For this reason, the actual trapping coefficient K depends on the target position inside the confining domain, namely, on r_T and z_T, and on the relative size of the target as compared to the cross section of the confining domain. The dependence on z_T is adiabatic and comes with the slowly changing profile of the domain, $r(z)$. As K should be an analytic function of r_T, it can be represented as a Taylor series in powers of r_T whose coefficients depend on the disk radius a. Moreover, K has a weak maximum at the center of the domain (the most symmetrical configuration) that follows from the symmetry of the problem and general bounds on the capacitance. As a consequence, there is no linear term in the Taylor series expansion. Truncating it up to the second-order term, we can use the simple ansatz

$$\Psi(\nu, \eta) \equiv \frac{K(\nu, \eta)}{K_0} = A(\nu)[1 - B(\nu)\eta^2], \tag{A1}$$

where $K_0 = 8aD$ is the trapping coefficient of a disk of radius a, $\eta = r_T/r(z_T) \leqslant 1$ is the offset of the disk with respect to the domain axis, $\nu = a/r(z_T) \ll 1$ is the relative size of the target with respect to the domain cross section at z_T, and coefficients $A(\nu)$ and $B(\nu)$ are to be determined.

For $\eta = 0$ (the centered disk) the solution has been derived by Fock [58], from which we have

$$A(\nu) = \frac{1 + 1.37\nu - 0.37\nu^4}{(1 - \nu^2)^2} \geqslant 1. \tag{A2}$$

The second parameter $B(\nu)$ can be found from the situation when the disk touches the wall of the tube. In this case $\eta = 1 - \nu$ and we can write this condition in the form

$$\frac{K}{K_0} = qA, \tag{A3}$$

with some constant factor q. The value of factor q can be deduced from a general scaling argument. It is well known that the capacitance (and hence the trapping rate) scales with the square root of the surface area of conductor (absorber) [39,44]. So the capacitance of any conductor touching the reflecting wall is approximately $\sqrt{2}/2 \approx 0.71$ of its value at the center of the tube (at $\eta = 0$), which leads to Eq. (A3). This conjecture can also be validated with the analytical results for two touching disks, $q = \frac{3}{4}$ [59] or $q = 0.74$ [60], and two touching spheres when $q = \ln 2 \approx 0.69$ [39,61], which are reasonably close. From here we arrive at

$$B(\nu) = \frac{1 - q}{(1 - \nu)^2} > 0. \tag{A4}$$

[1] S. Redner, *A Guide to First Passage Processes* (Cambridge University Press, Cambridge, 2001).

[2] *First-Passage Phenomena and Their Applications*, edited by R. Metzler, G. Oshanin, and S. Redner (World Scientific, Singapore, 2014).

[3] *Chemical Kinetics: Beyond the Textbook*, edited by K. Lindenberg, R. Metzler, and G. Oshanin (World Scientific, Hackensack, 2019).

[4] D. Reguera and J. M. Rubi, Kinetic equations for diffusion in the presence of entropic barriers, Phys. Rev. E **64**, 061106 (2001).

[5] Y. Lanoiselée, N. Moutal, and D. S. Grebenkov, Diffusion-limited reactions in dynamic heterogeneous media, Nat. Commun. **9**, 4398 (2018).

[6] D. S. Grebenkov, Paradigm Shift in Diffusion-Mediated Surface Phenomena, Phys. Rev. Lett. **125**, 078102 (2020).

[7] P. Bressloff and S. D. Lawley, Stochastically gated diffusion-limited reactions for a small target in a bounded domain, Phys. Rev. E **92**, 062117 (2015).

[8] M. Reva, D. A. DiGregorio, and D. S. Grebenkov, A first-passage approach to diffusion-influenced reversible binding: Insights into nanoscale signaling at the presynapse, Sci. Rep. **11**, 5377 (2021).

[9] D. S. Grebenkov, Universal Formula for the Mean First Passage Time in Planar Domains, Phys. Rev. Lett. **117**, 260201 (2016).

[10] O. Bénichou and R. Voituriez, From first-passage times of random walks in confinement to geometry-controlled kinetics, Phys. Rep. **539**, 225 (2014).

[11] P. Kalinay and J. K. Percus, Corrections to the Fick-Jacobs equation, Phys. Rev. E **74**, 041203 (2006).

[12] J. M. Rubi and D. Reguera, Thermodynamics and stochastic dynamics of transport in confined media, Chem. Phys. **375**, 518 (2010).

[13] A. E. Lindsay, A. J. Bernoff, and M. J. Ward, First passage statistics for the capture of a Brownian particle by a structured spherical target with multiple surface traps, SIAM Multiscale Model. Simul. **15**, 74 (2017).

[14] D. Holcman and Z. Schuss, *Stochastic Narrow Escape in Molecular and Cellular Biology* (Springer, Berlin, 2015).

[15] B. O. Koopman, *Search and Screening: General Principles with Historical Applications* (Pergamon, Oxford, 1980).

[16] O. Bénichou, C. Loverdo, M. Moreau, and R. Voituriez, Intermittent search strategies, Rev. Mod. Phys. **83**, 81 (2011).

[17] G. Oshanin, O. Vasilyev, P. L. Krapivsky, and J. Klafter, Survival of an evasive prey, Proc. Natl. Acad. Sci. USA **106**, 13696 (2009).

[18] O. Bénichou, D. S. Grebenkov, P. Levitz, C. Loverdo, and R. Voituriez, Optimal Reaction Time for Surface-Mediated Diffusion, Phys. Rev. Lett. **105**, 150606 (2010).

[19] O. Bénichou, C. Chevalier, J. Klafter, B. Meyer, and R. Voituriez, Geometry-controlled kinetics, Nat. Chem. **2**, 472 (2010).

[20] D. S. Grebenkov, R. Metzler, and G. Oshanin, Strong defocusing of molecular reaction times results from an interplay of geometry and reaction control, Commun. Chem. **1**, 96 (2018).

[21] I. V. Grigoriev, Y. A. Makhnovskii, A. M. Berezhkovskii, and V. Y. Zitserman, Kinetics of escape through a small hole, J. Chem. Phys. **116**, 9574 (2002).

[22] T. Kolokolnikov, M. S. Titcombe, and M. J. Ward, Optimizing the fundamental neumann eigenvalue for the laplacian in a domain with small traps, Eur. J. Appl. Math. **16**, 161 (2005).

[23] A. Singer, Z. Schuss, D. Holcman, and R. S. Eisenberg, Narrow escape, Part I, J. Stat. Phys. **122**, 437 (2006).

[24] A. Singer, Z. Schuss, and D. Holcman, Narrow escape, Part II: The circular disk, J. Stat. Phys. **122**, 465 (2006).

[25] A. Singer, Z. Schuss, and D. Holcman, Narrow escape, Part III: Riemann surfaces and non-smooth domains, J. Stat. Phys. **122**, 491 (2006).

[26] S. Pillay, M. J. Ward, A. Peirce, and T. Kolokolnikov, An asymptotic analysis of the mean first passage time for narrow escape problems: Part I: Two-dimensional domains, SIAM Multi. Model. Simul. **8**, 803 (2010).

[27] A. F. Cheviakov, M. J. Ward, and R. Straube, An asymptotic analysis of the mean first passage time for narrow escape problems: Part II: The sphere, SIAM Multi. Model. Simul. **8**, 836 (2010).

[28] A. F. Cheviakov and M. J. Ward, Optimizing the principal eigenvalue of the Laplacian in a sphere with interior traps, Math. Computer Model. **53**, 1394 (2011).

[29] A. F. Cheviakov, A. S. Reimer, and M. J. Ward, Mathematical modeling and numerical computation of narrow escape problems, Phys. Rev. E **85**, 021131 (2012).

[30] C. Caginalp and X. Chen, Analytical and numerical results for an escape problem, Arch. Ration. Mech. Anal. **203**, 329 (2012).

[31] D. Holcman and Z. Schuss, The narrow escape problem, SIAM Rev. **56**, 213 (2014).

[32] J. S. Marshall, Analytical solutions for an escape problem in a disc with an arbitrary distribution of exit holes along its boundary, J. Stat. Phys. **165**, 920 (2016).

[33] D. S. Grebenkov and G. Oshanin, Diffusive escape through a narrow opening: New insights into a classic problem, Phys. Chem. Chem. Phys. **19**, 2723 (2017).

[34] D. S. Grebenkov, R. Metzler, and G. Oshanin, Towards a full quantitative description of single-molecule reaction kinetics in biological cells, Phys. Chem. Chem. Phys. **20**, 16393 (2018).

[35] D. S. Grebenkov, R. Metzler, and G. Oshanin, Full distribution of first exit times in the narrow escape problem, New J. Phys. **21**, 122001 (2019).

[36] D. S. Grebenkov, R. Metzler, and G. Oshanin, Effects of the target aspect ratio and intrinsic reactivity onto diffusive search in bounded domains, New J. Phys. **19**, 103025 (2017).

[37] D. S. Grebenkov and A. T. Skvortsov, Mean first-passage time to a small absorbing target in an elongated planar domain, New J. Phys. **22**, 113024 (2020).

[38] P. L. Krapivsky, S. Redner, and E. Ben-Naim, *A Kinetic View of Statistical Physics* (Cambridge University Press, Cambridge, 2010).

[39] A. M. Berezhkovskii and A. V. Barzykin, Simple formulas for the trapping rate by nonspherical absorber and capacitance of nonspherical conductor, J. Chem. Phys. **126**, 106102 (2007).

[40] A. T. Skvortsov and A. M. Berezhkovskii, and L. Dagdug, Trapping of diffusing particles by spiky absorbers, J. Chem. Phys. **148**, 084103 (2018).

[41] P. R. Nair and M. A. Alam, Dimensionally Frustrated Diffusion towards Fractal Adsorbers, Phys. Rev. Lett. **99**, 256101 (2007).

[42] N. Landkof, *Foundations of Modern Potential Theory* (Springer, Berlin, 1972).

[43] L. D. Landau, L. P. Pitaevskii, and E. M. Lifshitz, *Electrodynamics of Continuous Media* (Elsevier, Amsterdam, 1984).

[44] Y. L. Chow and M. M. Yovanovich, The shape factor of the capacitance of a conductor, J. Appl. Phys. **53**, 8470 (1982).

[45] H. J. Wintle, The capacitance of the cube and square plate by random walk methods, J. Electrostat. **62**, 51 (2004).

[46] F. Piazza and D. S. Grebenkov, Diffusion-controlled reaction rate on non-spherical partially absorbing axisymmetric surfaces, Phys. Chem. Chem. Phys. **21**, 25896 (2019).

[47] M. J. Crocker, *Handbook of Acoustics* (Wiley, New York, 1998).

[48] S. Tretyakov, *Analytical Modeling in Applied Electromagnetics* (Artech House, Boston, 2003).

[49] D. P. Hewett and I. J. Hewitt, Homogenized boundary conditions and resonance effects in Faraday cages, Proc. R. Soc. A **472**, 20160062 (2016).

[50] J. J. Marigo and A. Maurel, Two-scale homogenization to determine effective parameters of thin metallic-structured films, Proc. R. Soc. A **472**, 20160068 (2016)

[51] P. A. Martin, On Green's function for Laplace's equation in a rigid tube, Q. Appl. Math. **80**, 87 (2022).

[52] C. W. Gardiner, *Handbook of Stochastic Methods for Physics, Chemistry and the Natural Sciences* (Springer, Berlin, 1985).

[53] V. G. Maz'ya, S. A. Nazakov, and B. A. Plamenevskii, Asymptotic expansions of the eigenvalues of boundary value problems for the Laplace operator in domains with small holes, Math. USSR. Izv. **24**, 321 (1985).

[54] M. J. Ward and J. B. Keller, Strong localized perturbations of eigenvalue problems, SIAM J. Appl. Math. **53**, 770 (1993).

[55] W. R. Smythe, Charged sphere in cylinder, J. Appl. Phys. **31**, 553 (1960).

[56] W. R. Smythe, Charged spheroid in cylinder, J. Math. Phys. **4**, 833 (1963).

[57] I. C. Chang, and I. D. Chang, Potential of a charged axially symmetric conductor inside a cylindrical tube, J. Appl. Phys. **41**, 1967 (1970).

[58] V. A. Fock, A theoretical investigation of the acoustical conductivity of a circular aperture in a wall put across a tube, Dokl. Akad. Nauk SSSR **31**, 875 (1941).

[59] V. I. Fabrikant, On the potential flow through membranes, Z. Angew. Math. Phys. **36**, 616 (1985).

[60] W. Strieder, Interaction between two nearby diffusion-controlled reactive sites in a plane, J. Chem. Phys. **129**, 134508 (2008).

[61] J. Lekner, Capacitance coefficients of two spheres, J. Electrostat. **69**, 11 (2011).